(Fig. 2f). This line was not observed in the spectrum of the exciting line. Its distance to the unshifted line was 0.09 - 0.13 $cm^{-1}$ at room temperature and increased slightly with rising temperature. The intensity of this line was strong enough to produce sometimes a SMBS component. When the exciting light flux was reduced to a value at which a broad section of the SRWS spectrum vanished, this sharp line still remained. It was further established that this line is a weak laser-emission mode,**** which becomes stronger in a medium with anisotropic molecules, by a mechanism which is practically the same as in SRWS. A similar effect was apparently observed recently by Cho et al. [6], who took it to be SRWS. The temperature dependence which they observed for the position of this line may be due to the temperature dependence of the gain and to a mechanism analogous to that indicated by Brewer for SMBS.


[1] D. I. Mash, V. V. Morozov, V. S. Starunov, and I. L. Fabelinskii, JETP Letters 2, 41 (1965), transl. p. 25.
[2] V. S. Starunov, Investigation of the Spectrum of Thermal and Stimulated Molecular Scattering of Light, Dissertation, Phys. Inst. Acad. Sci., 1965; Trudy FIAN (in press), 1967; DAN SSSR (in press).
[3] I. L. Fabelinskii, Molekulyarnoe rasseyanie sveta (Molecular Scattering of Light), Nauka, 1965.
[4] R. Chiao, P. Kelly, and E. Garmire, Phys. Rev. Lett. 17, 1158 (1966).
[5] D. I. Mash, V. V. Morozov, V. S.Starunov, E. V. Tiganov, and I. L. Fabelinskii, JETP Letters 2, 246 (1965), transl. p. 157.
[6] C. W. Cho, N. D. Foltz, D. H. Rank, and T. R. Wiggins, Phys. Rev. Lett. 18, 107 (1967).
[7] R. G. Brewer, Appl. Phys. Lett. 9, 51 (1966).


*The first SMBS component may appear in the scattered-light spectrum as a result of reflection from the vessel windows, ruby end faces, etc.

**When the laser emission was focused with a lens of f = 2.5 cm, we observed in nitrobenzene and o-xylol both the Stokes and anti-Stokes parts of the wing in several orders of the interference patterns, and only the Stokes wing in the remaining orders. We assume that in this case we observed four-photon interaction with SRWS at angles $\theta < 2^\circ$.

***This line can be seen in Fig. 1 of [5] between the exciting line and the SMBS component.

****When the distance between the laser resonator surfaces is changed by a factor 1.5, the distance between this line and the main mode of emission changes by the same factor.

## NONLINEAR DEFOCUSING OF LASER BEAMS


S. A. Akhmanov, D. P. Krindach, A. P. Sukhorukov, and R. V. Khokhlov
Physics Department, Moscow State University


Submitted 4 May 1967
ZhETF Pis'ma 6, No. 2, 509-513 (15 July 1967)


1. We report in this letter the results of a theoretical and experimental investigation of the phenomenon of nonlinear defocusing (principal attention was paid to the steady-state operation) of cw laser beams in liquids. This phenomenon is ocnnected with the dependence of the refractive index on the intensity of the optical field, which is of the form $n = n_0 + n_2|E^2|$. Low-inertia nonlinearity mechanisms with $n_2 > 0$ lead to self-focusing of powerful short pulses [1,2]. For cw lasers, inertial mechanisms are significant, primarily heating of the medium. For this mechanism usually $n_2 < 0$ and defocusing of the beam results; some data on this effect are reported in [6], where it was investigated in an He-Ne laser, and in [7], where only the registration of the effect is reported.

We present below the results of experiments with an argon laser; these reveal the main dependences of the defocusing effect on the beam parameters and on the properties of the liquid.

2. The series of experiments in which we registered the change in the divergence of the laser beam was performed with an argon laser with a dispersion resonator, at a wavelength 4880 Å. The initial laser-beam divergence was $\theta_0 = 2.5'$, the beam radius at the output mirror was $a_0 = 0.06$ cm, and the maximum power was $P_{max} \approx 0.15$ W. A cylindrical cell with plane-parallel windows was filled with the investigated liquid (water, acetone, or alcohol) and placed in the path of the laser beam. The lengths $\ell$ of the different cells ranged from 10 to 84 cm, and their radii R from 1.5 to 2.5 cm. Addition of a small amount of soluble absorber made it possible to vary the absorption in the liquids between sufficiently wide limits, from $\delta^{-1} \approx 10$ cm to $\delta^{-1} \approx 10^3$ cm.

The results of experiments performed for different values of $P_0$, $\ell$, $\delta$, and a/R have

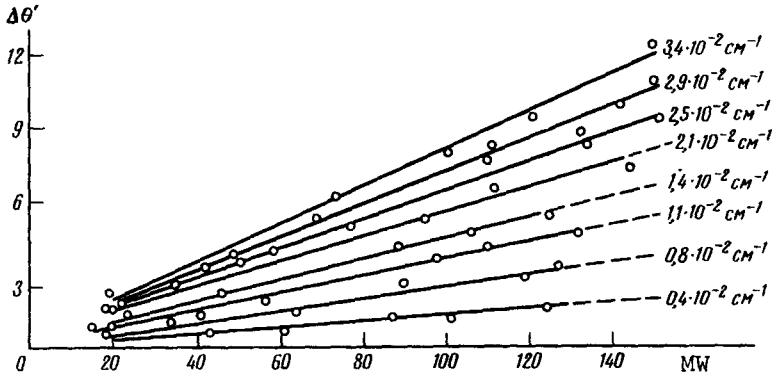


Fig. 1. Experimental plot of increase of beam divergence of argon laser, after passing through a cell with water, vs. power at entrance to cell. R/a = 30. The parameter of the curves is the power absorption coefficient $\delta$. The cell parameters are $\ell$ = 44 cm, diam = 48 mm, V = 820 cc.

shown that the laws governing the defocusing are the same for the investigated liquids. They are illustrated in Figs.1 and 2, which were obtained for water in a stationary defocusing regime. We see that the thermal defocusing $\Delta\theta$ increases linearly with the power $P_0$. In the case of large absorption ($\delta\ell \to \infty$) the value of $\Delta\theta$ tends to a limit $\Delta\theta_{lim}$. In practice it is more convenient to determine the latter from the linear plots of the defocusing vs. the fraction of the energy absorbed in the liquid, $\Delta\theta = f(\exp(-\delta\ell))$. By moving the cell to different distances from the laser it was established that the nonlinear defocusing $\Delta\theta$ is inversely proportional

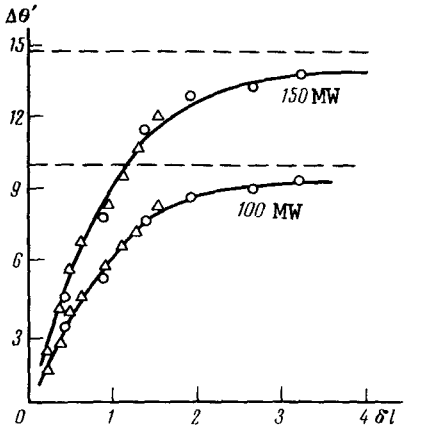


Fig. 2. Plots of increase of beam divergence of argon laser, after passing through a cell with water, vs. the reduced optical-path length $\delta\ell$. The parameter of the curves is the beam power entering the cell. The dashed lines denote the limiting defocusing corresponding to the given power values. The circles and triangles correspond to cells 84 and 44 cm long, respectively.

to the radius of the beam at the entrance to the cell. The experimental results and the calculated data are summarized in the table.

| Liquid | $\frac{\partial n}{\partial T}$, $deg^{-1}$ | $\kappa$, W/cm-deg | $P_0$, W | $a$, cm | Limiting defocusing | |
|---|---|---|---|---|---|---|
| | | | | | $\Delta\theta_{lim}^{exp}$, min | $\Delta\theta_{lim}^{theor}$, min |
| Water | $0.8\cdot10^{-4}$ | $6\cdot10^{-3}$ | 0.10 | 0.09 | 10.0±0.7 | 12.0 |
| | | | 0.15 | 0.09 | 14.8±0.7 | 18.2 |
| | | | 0.15 | 0.16 | 9.0±0.7 | 10.3 |
| Acetone | $5\cdot10^{-4}$ | $1.6\cdot10^{-3}$ | 0.10 | 0.07 | 28 ± 1.5 | 34.5 |
| | | | 0.15 | 0.07 | 41 ± 1.5 | 51.5 |
| Alcohol | $4\cdot10^{-4}$ | $1.7\cdot10^{-3}$ | 0.10 | 0.07 | 20.5±1.5 | 26 |
| | | | 0.15 | 0.07 | 30.5±1.5 | 37.5 |

3. The theory of thermal defocusing of a light beam is based on a simultaneous solution of the equations of thermal conductivity and of the wave equation.

The solution of the nonstationary equation of thermal conductivity for a medium heated by a Gaussian beam $A\exp(-r^2/a^2)$ shows that the transverse temperature gradient is given by

$$\frac{\partial T'}{\partial r} = \frac{P\delta}{2\pi n_0 \kappa r}\left[\exp\left(-2r^2/a^2\right) - \exp\left(-2r^2/a^2(1+tr^{-1})\right)\right], \qquad (1)$$

where $\kappa$ is the coefficient of thermal conductivity of the medium, $\tau = a^2\rho c_p/\delta\kappa$ is the characteristic time of establishment of the stationary temperature gradient, and $\rho c_p$ is the specific heat per unit volume. We note that the process of establishment of the average temperature in the cell is slower and is determined by the influence of the cell walls.

The appearance of a temperature gradient leads to optical inhomogeneity of the medium ($n = n_0 + \partial n/\partial T\, T'$) and, as a result to nonlinear refraction. It follows from (1) that the nonlinear defocusing of a Gaussian beam is accompanied, in general, by aberrations (the increment of the refractive index is not quadratic in r). At sufficiently small powers, and consequently small temperature gradients, the defocusing can in first approximation be regarded as free of aberrations; then the Gaussian beam retains its shape. Using the procedure developed by us for the calculation of self-focusing [3], we can write for the stationary* case ($t \gg \tau$), in the geometric-optics approximation, the following equation

$$\frac{\partial^2 f}{\partial z^2} = \frac{\frac{\partial n}{\partial T} P_0 \delta \exp(-\delta z)}{\pi n_0^2 a_0^2 \kappa f} \qquad (2)$$

for the dimensionless beam width f; the quantity $\theta = n_0 a_0 f'$ characterizes the divergence of the beam in a given section z. Assuming that in the region of effective nonlinear defocusing the intensity is altered essentially as a result of absorption, we obtain by integrating (2) the following expression for the beam divergence over a path length $\ell$:

$$\theta = \theta_0 + \frac{\frac{\partial n}{\partial T} P_0}{\pi n_0 a_0 \kappa} [1 - \exp(-\delta \ell)] \tag{3}$$

It follows from (3) that as $\delta \ell \to \infty$ there is formed a limiting nonlinear divergence

$$\Delta \theta_{\text{lim}} = \frac{\frac{\partial n}{\partial T} P_0}{\pi n_0 a_0 \kappa} \tag{4}$$

The theoretical plots of (3) and the values of $\Delta\theta_{\text{lim}}$ are shown in Figs. 1 and 2 and in the table. The quantitative agreement with experiment is good.

At high power, the temperature gradient increases and nonlinear aberrations appear in the "thermal" lens. These are observed first in the far field, and then in the cell itself. The point is that with increasing distance from the beam axis, the slope of the rays ($\theta \sim \partial T/\partial r$) first increases (as in a spherical wave), but then when $r > a$ the slope decreases. This causes the rays to cross and to interfere. The most distinct interference picture is observed when the rays have approximately identical intensity, i.e., in the region of maximum deflection angle (near the edge of the beam). As a result, as $P_0$ is increased, there appears first in the cross section of the beam one round ring, followed by a whole series of less distinct rings (see [3] concerning the calculation of the nonlinear aberrations in self-focusing). The picture of nonlinear aberrations was clearly observed in the experiments for a specified power level, and became more distinct with increasing $\Delta\theta_{\text{lim}}$ (see Fig. 3). It must be emphasized at

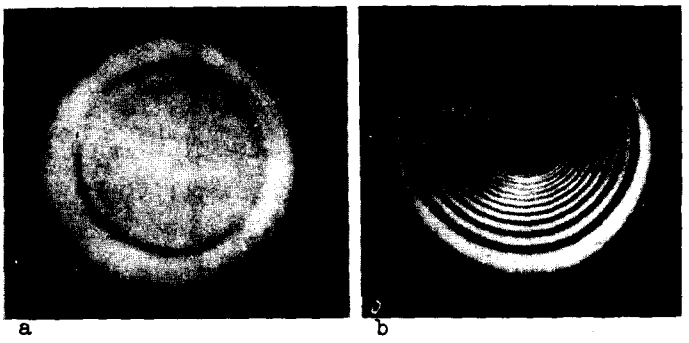


Fig. 3. Aberration rings produced in the cross section of an argon-laser beam upon passage through a 10 cm cell with a solution of fuchsine in alcohol ($\delta$ = 0.18 $cm^{-1}$). The power entering the cell is 6 MW (a) or 60 MW (b).

the same time that the experimentally observed beam divergences lie well on the lines of Fig. 1 even in the presence of aberrations.

4. The effect of nonlinear defocusing may give way, obviously, to the self-focusing effect in media with $\partial n/\partial T > 0$ [4]. Although it is difficult to produce in gas-laser beams conditions for beam collapse, the effect of a certain nonlinear compensation of the initial divergence can be produced. We succeeded in observing a decrease in laser-beam divergence by an amount $\Delta\theta_{\text{lim}}$ (see (4)) in optical glass. An interesting question is that of defocusing of compound beams; its theoretical analysis can be performed by perturbation theory. It turns out then that, just as in the case of self-focusing [8], there exists a transverse perturbation scale leading to the fastest defocusing.

[1] G. A. Askar'yan, JETP 42, 1567 (1962), Soviet Phys. JETP 15, 1088 (1962).
[2] R. Chiao, E. Garmire, and C. Townes, Phys. Rev. Lett. 13, 479 (1964).
[3] S. A. Akhmanov, A. P. Sukhorukov, and R. V. Khokhlov, JETP 50, 1537 (1966), Soviet Phys. JETP 23, 1025 (1966).
[4] A. G. Litvak, JETP Letters 4, 341 (1966), transl. p. 230.
[5] Yu. P. Raizer, JETP 52, 470 (1967), Soviet Phys. JETP 25, 308 (1967).
[6] J. Gordon, R. Leite, R. Moore, S. Porto, and J. Whinnery, J. Appl. Phys. 36, 3 (1965).
[7] K. Rieckhoff, Appl. Phys. Lett. 9, 87, (1966).
[8] V. I. Bespalov and V. I. Talanov, JETP Letters 3, 471 (1966), transl. p. 307.

*See [5] concerning nonstationary defocusing.

## CERTAIN FEATURES OF THE BEHAVIOR OF p-InSb SAMPLES WITH UNCOMPENSATED ACCEPTOR DENSITY $6 \times 10^{11} - 1 \times 10^{14}$ cm$^{-3}$

F. F. Kharakhorin, M. F. Poluboyarinova, and V. G. Vinogradova
Submitted 5 May 1967
ZhETF Pis'ma 6, No. 2, 513-517 (15 July 1967)

Great interest has been shown in recent investigations of the properties of p-type indium antimonide in the question of the nature and location of the energy levels of the impurities, particularly of the so-called deep level. Several investigations have already been devoted to the observation of the deep level of p-type indium antimonide [1-5]. However, there is no unified point of view regarding the nature and character of this level as yet. One can hope that an increase in the scope of the research (with respect to the temperature, the carrier density, the number of doping acceptor elements) will uncover new approaches to the solution of this problem.

We have measured the temperature dependences of the Hall constant and the electric-conductivity and mobility coefficients of compensated (90% degree of compensation) samples of p-type indium antimonide with resistivities from 10 to 2740 ohm-cm and with low density of uncompensated holes ($6 \times 10^{11} - 1 \times 10^{-4}$ cm$^{-3}$) in the interval from 4.2 to 300°K. The single crystals were doped with acceptor impurities (manganese, silicon, germanium, gold) during the course of drawing by the Czochralski method.

The temperature dependence of the hole density, defined as $p = 1/Re_c$, was investigated in more than 40 samples in the 55 - 130°K range. It has turned out that, regardless of the method used to obtain the sample and the nature of the doping impurity, the deep level is observed (we have in mind the corresponding inclinations of curves 1-5 of Fig. 1 in the temperature interval 78 - 110°K) only in samples with carrier density $p = 6 \times 10^{11} - 7 \times 10^{13}$ cm$^{-3}$. This level is not observed at higher densities of the uncompensated holes (curves 6 and 7 of Fig. 1). The activation energy of the deep level fluctuates in the range from 0.01 to 0.1 eV, depending on the carrier density. The fact that the activation energy of the deep level is independent of the doping impurity (Fig. 2) suggests that this level is caused by lattice defects.

Unlike [1-5], we measured samples with very low uncompensated-hole densities ($6 \times 10^{11} - 6 \times 10^{12}$ cm$^{-3}$), and this has made it possible to observe a unique variation of the Hall constant and of the mobility coefficient with temperature, wherein, regardless of the kind of doping impurity: 1) samples with hole density on the order of $6 \times 10^{11} - 6 \times 10^{12}$ cm$^{-3}$ have a clearly